Process and Refining Characteristics of ESR using MgO containing Slag Systems

S. Radwitz[1], H. Scholz[2], B. Friedrich[1], H. Franz[2]

[1]IME Process Metallurgy and Metal Recycling, RWTH Aachen University
[2]ALD Vacuum Technologies GmbH

sradwitz@ime-aachen.de

Abstract.The influence of selected process parameters such as slag composition, melt rate or pressure on metal-slag interactions, inclusion characteristics and process behaviour during electroslag remelting (ESR) are currently under investigation at IME, RWTH Aachen University. It is common knowledge that one of the main refining functions of ESR is the removal of non-metallic inclusions (NMI) to increase mechanical properties of the remelted material. On the other hand, metal-slag interactions can lead to continuous changes of alloying (e.g. Al, Si, Mn) and detrimental elements (O, S) with increasing ingot length and weight. This paper focuses on the influence of MgO addition to a common ESR slag system and the consequences regarding behaviour of process parameters such as electrical resistance, current density and power input as well as the modification of NMI characteristics, distribution of dissolved impurities and changes of alloying elements due to metal-slag interactions. In order to investigate the described correlations electrodes (110 mm diameter) of low alloyed steel (21CrMoV5-7) were remelted in a closed 400 kW-lab scale ESR furnace applying 1 bar protective argon atmosphere. Based on a widely used ESR slag composition consisting of approx. 60 wt.-% CaF_2, 19 wt.-% CaO, 19 wt.-% Al_2O_3 and 2 wt.-% MgO, pure magnesia was added in order to adjust the MgO content to 5, 10 and 15 wt.-% respectively. After remelting, the ingots as well as the electrode tips, which were immersed in the slag, were subjected to various chemical and structural characterisation methods. The concentration of basic and alloying elements over the ingot height and radius was determined by using optical emission spectroscopy. Interstitially dissolved elements were characterized by applying combustion and inert gas fusion methods. The amount, size, area and composition of non-metallic inclusions were investigated by metallographic methods as well as using SEM-EDX.

1. Introduction

Due to its utilization for manufacturing of special alloys such as high grade steels, the ESR process is one of the most important processes within special metallurgy. Despite the fact, that the advantages of remelted compared to conventional produced material are described for a lot of applications, the ESR process is still subject of numerous scientific studies due to the high amount of complex interrelations of all actuating variables with respect to refining and economic efficiency. Within this context, especially the composition of the slag systems used plays an important role regarding the removal of impurities and the adjustment of electrical parameters.
The results presented in this work are the continuation of the research work presented in [1] focusing on the influence of various slag compositions on refining and process characteristics for ESR steels.

2. Fundamentals

In the ESR process a consumable electrode is continuously remelted via a liquid slag in a water-cooled copper mould. The basic principle of the process in the stationary remelting phase is illustrated in Figure 1. As a result of the flow of electric current from the electrode via the liquid slag bath over the remelted ingot into the base plate and due to the fact that liquid slags show much higher electrical resistivities than metallic conductors, most of the applied electric power is transferred into heat in the slag bath. When the temperature of the slag bath exceeds the liquidus temperature of the electrode material, a thin film of liquid metal forms at the electrode tip from which droplets are continuously detached. Due to the density difference, the metal droplets sink through the slag and are collected in a liquid metal pool before solidification. [1], [2]

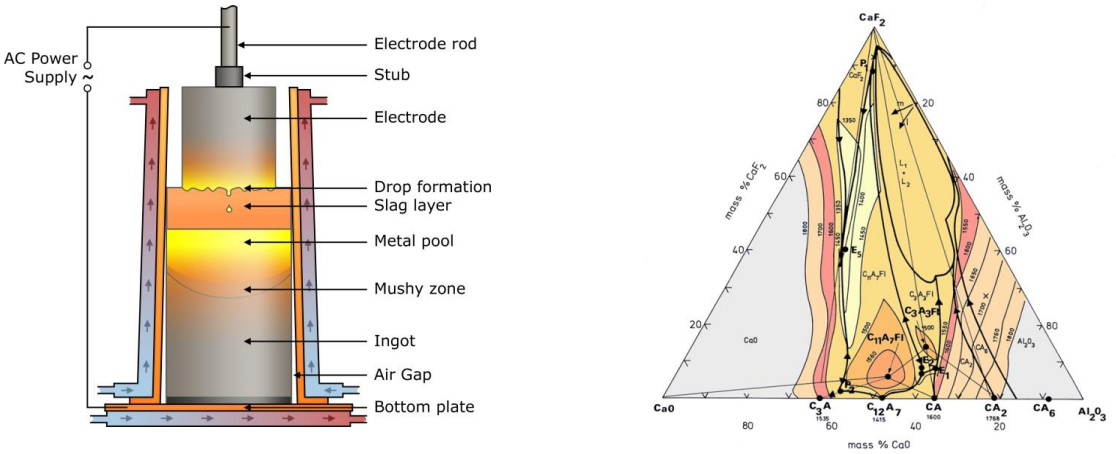

Figure 1. Schematic procedure of the ESR process (left) after [3] and ternary phase diagram of the most common ESR slag system CaF_2-CaO-Al_2O_3 (right) after [4]

With regard to ingot cleanliness and process control, the composition of the slag system used plays an important role. Most of the common slags which are utilized in the ER process consist of mixtures within the ternary system CaF_2-CaO-Al_2O_3, illustrated in Figure 1. Especially equal proportions of CaO and Al_2O_3 ensure low liquidus temperatures and therefore a satisfactorily melting behavior. Beside these standard constituents, MgO, SiO_2 or TiO_2 could be added to modify certain slag properties, e.g. with regard to metal-slag interactions, electrical resistance, liquidus temperature, viscosity or slag skin formation.

The addition of magnesia to conventional slag components is common procedure in industrial operation but in contrast to the influence of SiO_2 or TiO_2 on the aforementioned slag properties, not much information has been published.

Investigations of the electrical conductivity of the ternary system CaF_2-CaO-MgO have been carried out by Korp et al. [5] Within that study the amount of MgO was limited to 15 wt.-%, assuming that higher contents could enable the formation of stable periodic arcs which increase the risk of mold damage. A conductivity-lowering effect was observed with increasing MgO fraction which was much more distinct when compared to the influence of CaO but considerably lower as the influence of Al_2O_3. Regarding the removal of non-metallic inclusions (alumina and spinel inclusions), Salt [6] was able to record satisfactorily results using a slag consisting of 60 wt.-% CaF_2, 30 wt.-% CaO and 10 wt.-% MgO whereas Bhat [7] does not advise the slag system 80 wt.-% CaF_2, 11 wt.-% CaO and 9 wt.-% MgO due to the unstable formation of voltage and current. This phenomenon is also observed by Mitchell [8] who explains these instabilities by the formation of small quantities of Mg vapor during cathodic polarization of electrode and liquid metal pool. Especially, concentrations in the range of 10 wt.-% are considered as critical.

3. Experimental

In the present study four electrodes of a high-temperature steel 21CrMoV5-7 were remelted in a closed ESR furnace at IME, RWTH Aachen University using various slag compositions. With an average length of 1 100 mm and a diameter of 110 mm the electrode weights were around 84 kg. The utilized ESR furnace is able to operate at maximum 400 kW melting power at 50 Hz under defined atmospheric conditions up to 50 bar.

In order to investigate the influence of magnesia addition at constant amount of CaF_2 as well as fixed ratio of CaO/Al_2O_3 on the behavior of electrical parameters at a set melt rate and simultaneously on the refining capability with regard to oxygen, sulphur and non-metallic inclusions, four slag compositions with a successive increase of MgO were used for remelting. The desired slag compositions were obtained by mixing technical pure, pre-fused fluorspar and calcium-aluminate as well as an appropriate addition of pure magnesia. Denoted in the following order (CaF_2/CaO/MgO/Al_2O_3) the four idealized slag systems used were (60/19/2/19), (60/17,5/5/17,5), (60/15/10/15) and (60/12,5/15/12,5). The detailed compositions of the used slags are listed in Table 1.

Table 1. Slag compositions used for remelting

component / wt.-%	1	2	3	4
CaF_2	59,34	59,34	59,34	59,34
CaO	18,98	17,48	15,05	12,62
Al_2O_3	18,64	17,13	14,69	12,25
MgO	2,03	5,07	9,98	14,89
SiO_2	0,22	0,01	0,03	0,04
FeO	0,046	0,04	0,04	0,03

To minimize temperature affected differences with regard to metal-slag interactions, the melt rate was kept constant in all trials at 1.1 kg/min. Additionally, the immersion depth of the electrodes into the liquid slag bath were kept constant by using swing control. To minimize the influence of atmospheric oxygen, remelting was carried out at a slight overpressure (1.2 bar) argon atmosphere.

After remelting, the bulk slag, slag skin and flew dust were collected for mass balancing, measuring the slag skin thickness und for chemical analysis. The obtained ingots were cut into various sections (see Figure 2) which were subjected to several analyzing methods, as described in [1].

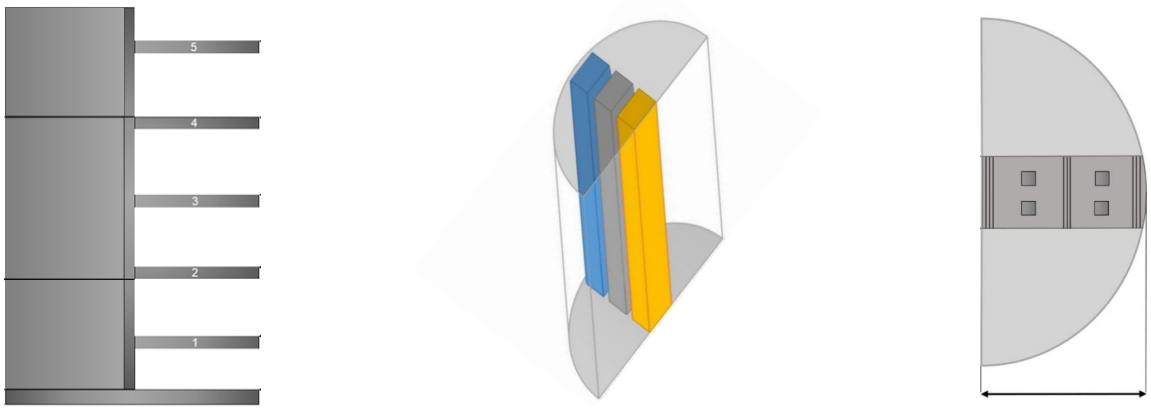

Figure 2. Schematic illustration of sample extraction from the remelted ingots

As described in [1] longitudinal discs from the ingot center were used to visualize the macro structure and to obtain information about the depth and shape of the liquid metal pool (see Figure 2, left). Stripes from the bottom, middle and top part were used for analyzing the matrix composition over the ingot height and radius (see Figure 2, middle) using optical emission spectroscopy. Additionally, from five horizontal extracted discs stripes for determining O, S, C, N and H by combustion and inert gas fusion methods were taken from positions at the ingot center, half radius and at the surface (radius). Furthermore, microstructure and distribution of non-metallic inclusions were characterized by light microscopy and SEM-EDX at two positions close to the ingot center and surface. The corresponding samples were extracted between the stripes for gas analysis (see Figure 2, right).

4. Results and Discussion

After each trial the recorded process data were evaluated and average values for power input, electrical resistance, voltage and current were built for the stationary remelting phase. In this context it should be noted that no mentionable irregularities after the starting phase were observed and all ingots were produced under constant remelting conditions. Figure 3 illustrates the correlation between electrical parameters and an increasing amount of MgO which is equivalent to a decrease of CaO and Al_2O_3. Thus, the observed decrease of electrical resistance with rising MgO amount is mainly a result of the reduced content of Al_2O_3 since this component strongly dominates the electrical resistance of the slag system. In contrast to that, the applied voltage, current and power are increasing until 10 wt.-% of MgO but start decreasing when more magnesia is added.

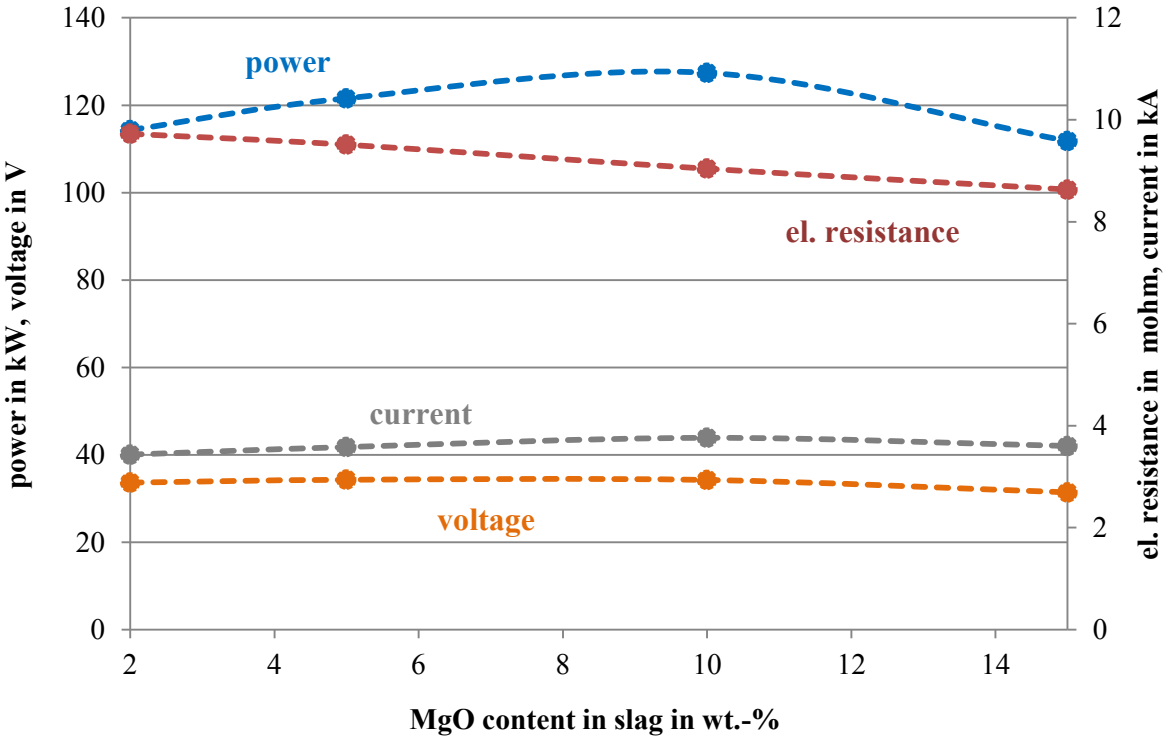

Figure 3. Correlation between the MgO content of the slag and selected process parameters

In addition to the logged process data the specific energy consumption (kWh/kg) was calculated which is illustrated in Figure 4. It is visible, that less energy is needed with increasing MgO amount in the slag to maintain the same melt rate of 1.1 kg/min.

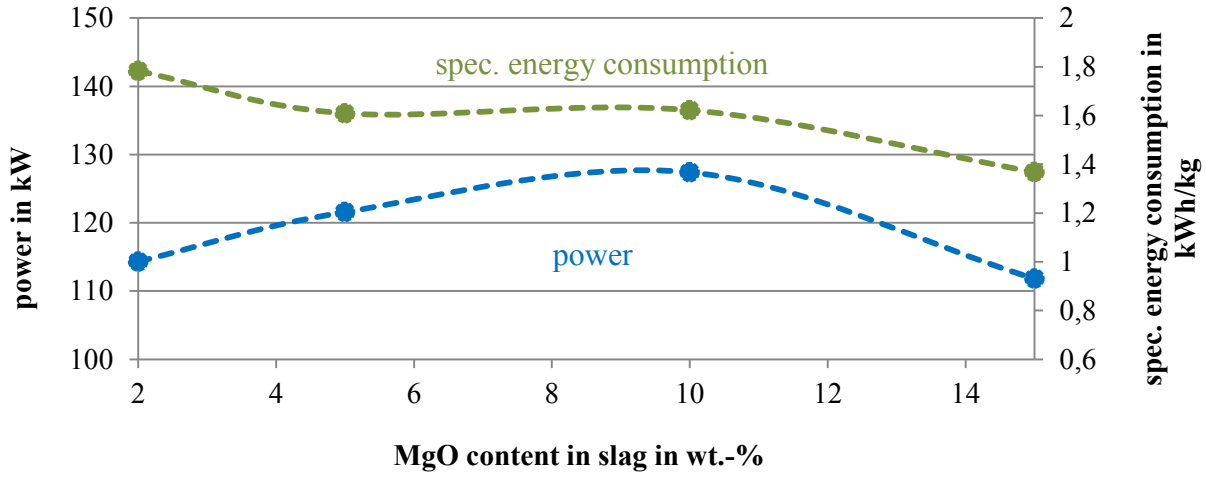

Figure 4. Dependency between specific energy consumption, supplied power and the amount of MgO in the slag

Beside the impact of electrical resistance on the applied current and power input, the heat loss to the water cooled copper mold also influences the necessary amount of supplied power. The correlation between supplied melting power and thickness of the formed slag skin is shown in Figure 5. The inverse trend is clearly visible what confirms the strong influence of slag skin thickness on heat extraction and the correlated power supply.

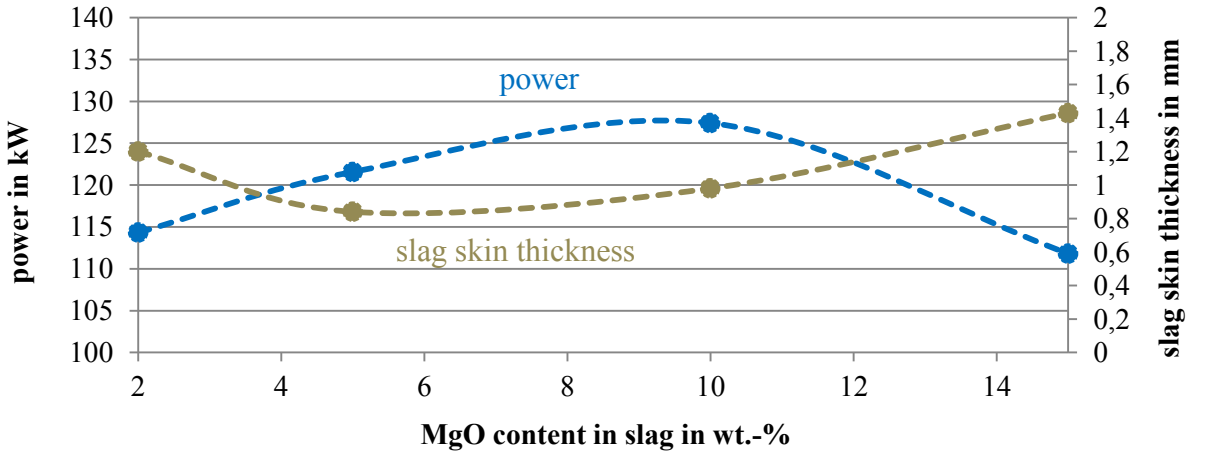

Figure 5. Applied power and thickness of the formed slag skin depending on slag composition

Referring to the behavior of base- and alloying elements, only for the contents of aluminum and silicon differences between ingot and electrode values were detected. The amounts of further alloying elements, e.g. chromium, vanadium or molybdenum did not show any changes when compared to the electrode contents or any variations over the ingot height It could be summarized that remelting under all utilized slag systems resulted in a pick-up of aluminum and a silicon loss. The corresponding trends over the ingot height for the various slag systems are illustrated in Figure 6 and Figure 7. Regarding the pick-up of aluminum, the highest amounts were obtained at the ingot bottom. With proceeding process time less Al was found in the metal but the ingot contents always exceeded electrode values. Furthermore, slight lower aluminum amounts were achieved by increasing the amount of MgO to 15 wt.-% which is equivalent to a reduction of the Al_2O_3 proportion to 12.5 wt.-%. Remelting under all other slag systems resulted in equal distributions of Al over the ingot height.

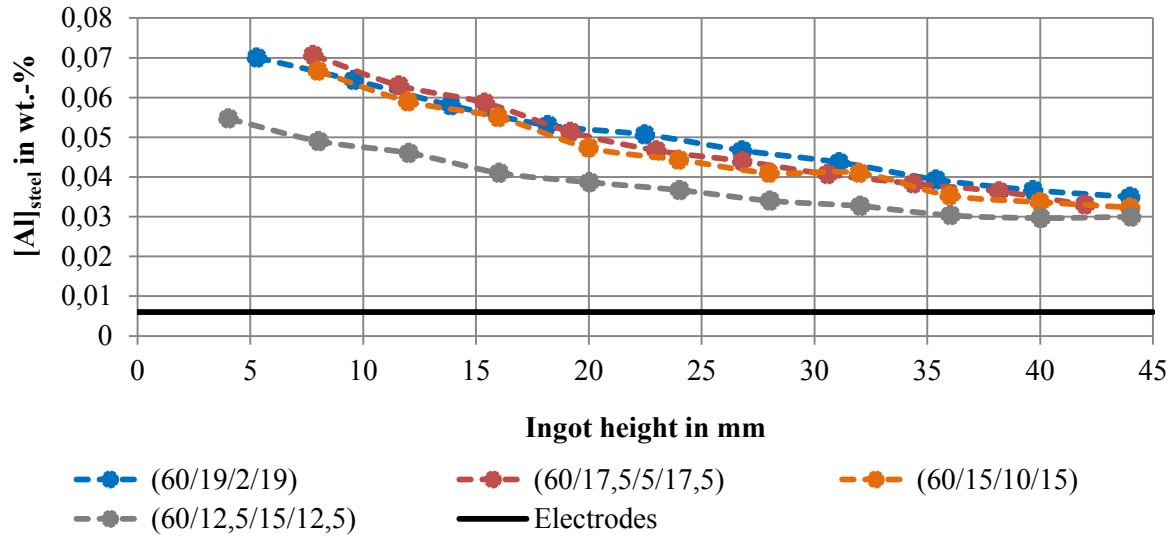

Figure 6. Behavior of aluminum dissolved in the remelted steel in correlation to slag composition

Regarding the detected silicon loss, no differences in the remelted material were found while slag composition was changed. It is noticeable, that in contrast to the trend of aluminum, the silicon loss was highest at the ingot bottom and reduced over the ingot height.

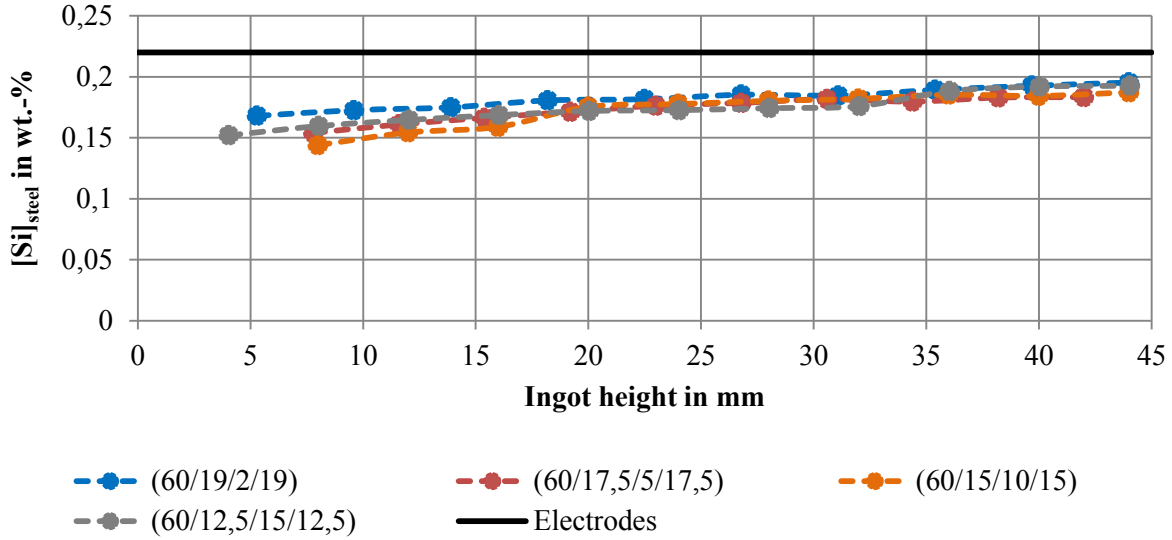

Figure 7. Development of silicon contents in the remelted steel depending on process slag composition

The obtained distributions of aluminum and silicon clearly demonstrate the metal-slag interaction due to the low activity of SiO_2 and high activity of Al_2O_3 in the slag, accompanied by the high activity of silicon and low activity of aluminum in the metal at process start. The approach to chemical equilibrium between slag- and steel-melt subsequently results in reduced silicon losses and aluminum pick-up with ongoing remelting time and ingot height, respectively (see Reaction 1).

$$3\,[Si]_{steel} + 2\,[Al_2O_3]_{slag} \leftrightarrow 2\,[Al]_{steel} + 3[SiO_2]_{slag} \quad (1)$$

In contrast to the variation of aluminum and silicon contents, no changes of total oxygen (T.O.) over the ingot length were found, despite different deoxidizing abilities of aluminum and silicon. It is further recognizable, that the oxygen levels in the remelted material are in the range of electrode values or even slightly higher and could not be significantly reduced. Figure 8 shows the content of total oxygen after remelting under the various slag compositions over the ingot height. The average amount of total oxygen for the electrodes is highlighted black whereas the range of measured oxygen values in the electrodes is illustrated grey.

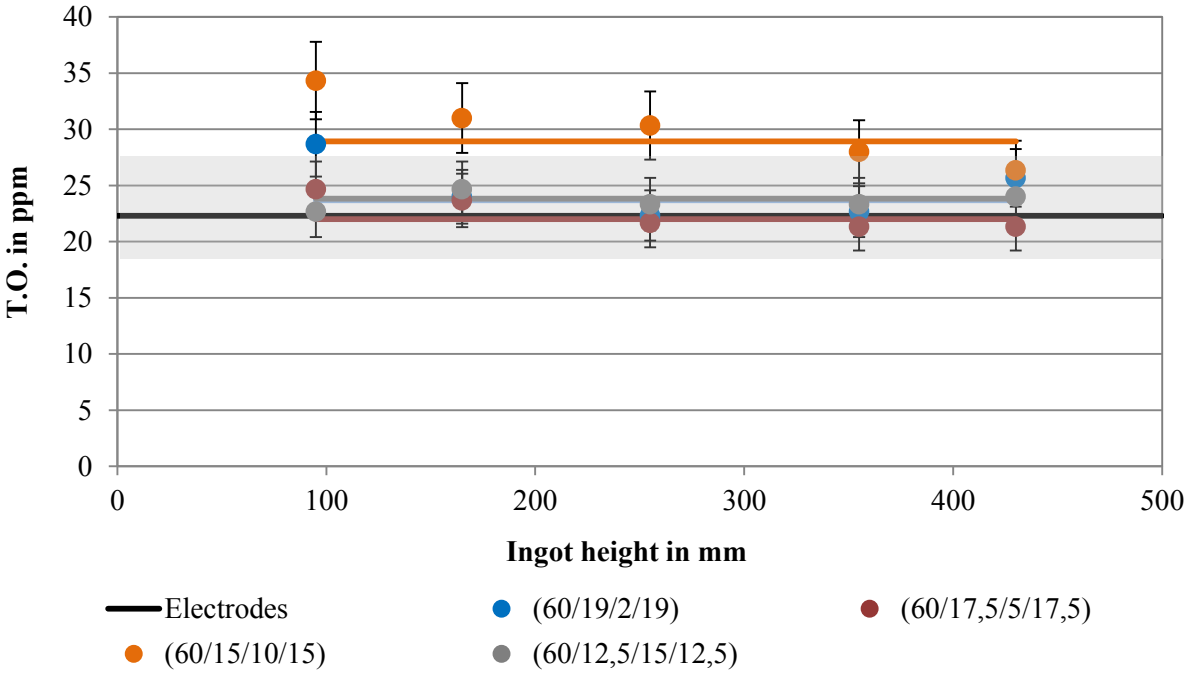

Figure 8. Content of total oxygen after remelting under various slags over the ingot height

The comparison of average total oxygen amounts depending on the amount of MgO is given in Figure 9. It could be seen, that the oxygen level is not strongly influence by the variations in slag composition, only slightly higher contents are detected at 10 wt.-% MgO.

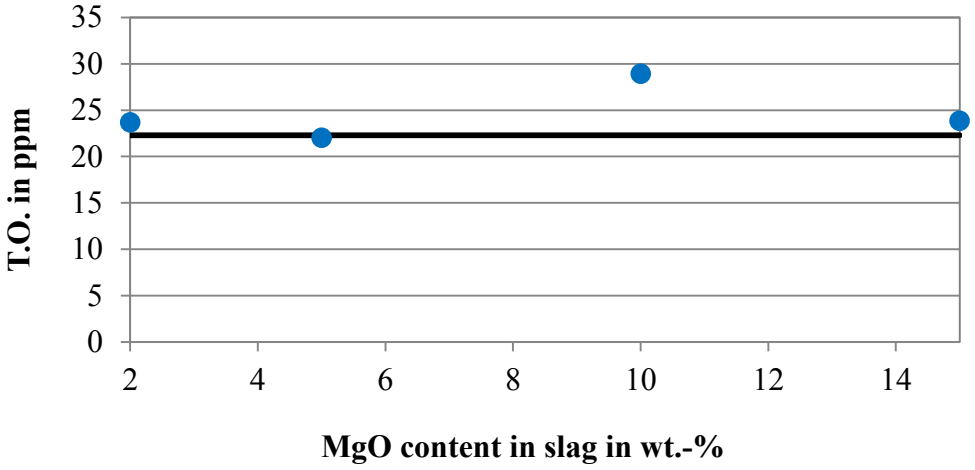

Figure 9. Correlation between total oxygen and slag composition

Desulphurization was successfully performed and no differences for desulphurization capability were found for the investigated composition range of slag systems. Since desulphurization in the ESR process under protective atmosphere is mainly based on the formation of CaS, slightly of MgS and the subsequent solution in the slag, desulphurization capability is reduced with proceeding process time. Therefore, the sulphur contents obtained in the remelted ingots slightly increase from approximately 10 to 18 ppm over the ingot height but are always significantly lower when compared to the input material (see Figure 10). In Figure 10, the average amount of total sulphur (T.S.) for the electrodes is highlighted black whereas the range of all measured electrode sulphur values is illustrated grey.

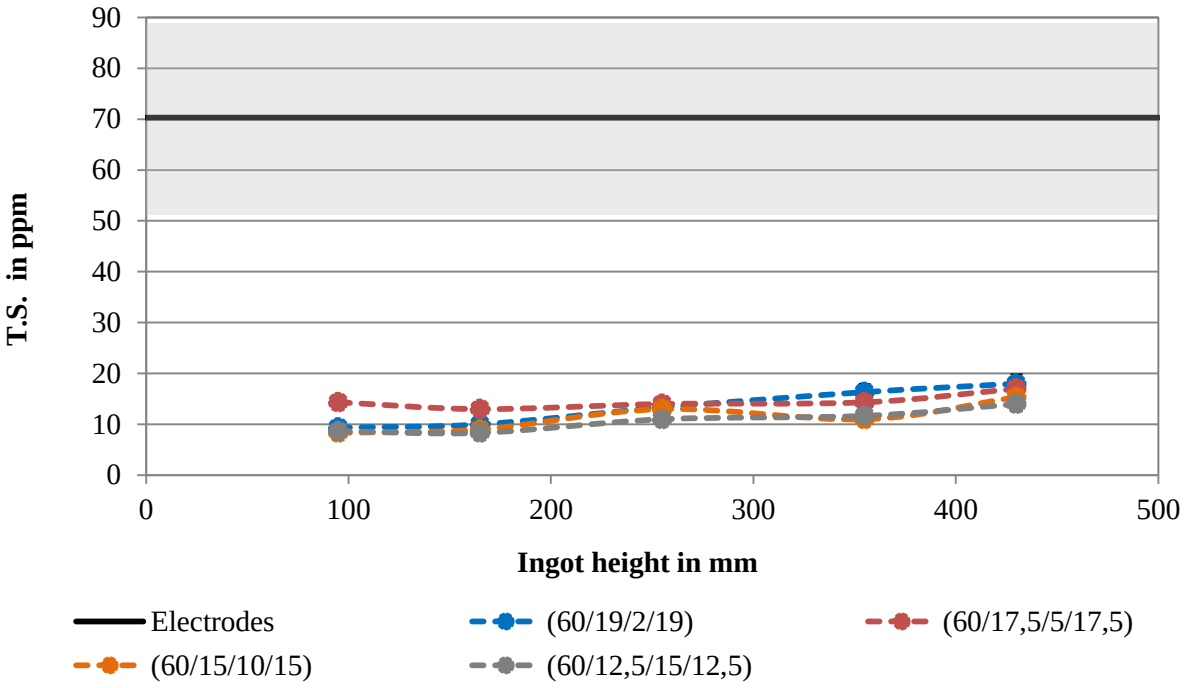

Figure 10. Development of sulphur contents in the remelted ingots for various slag systems

A characteristic image of a polished sample for inclusion investigation by light microscopy is shown in Figure 11 (right). By using this method, information about the number, size and the total area of inclusions were gained. Figure 11 (left) shows the determined class-divided number of inclusions per mm² depending on the amount of MgO in the slag. It could be seen, that large inclusions could be successfully removed. With regard to inclusions between 4 and 16 µm diameter, the slag system where no magnesia was added (60/19/2/19) results in a slightly lower cleanliness level since inclusions of 12 to 16 µm diameter are only found in the corresponding ingot. When MgO was added as slag component, the maximum inclusion diameter detected was < 12 µm. In contrast to the described behavior, the number of small inclusions (< 4µm) increased with rising amounts of MgO and even exceeded the electrode number.

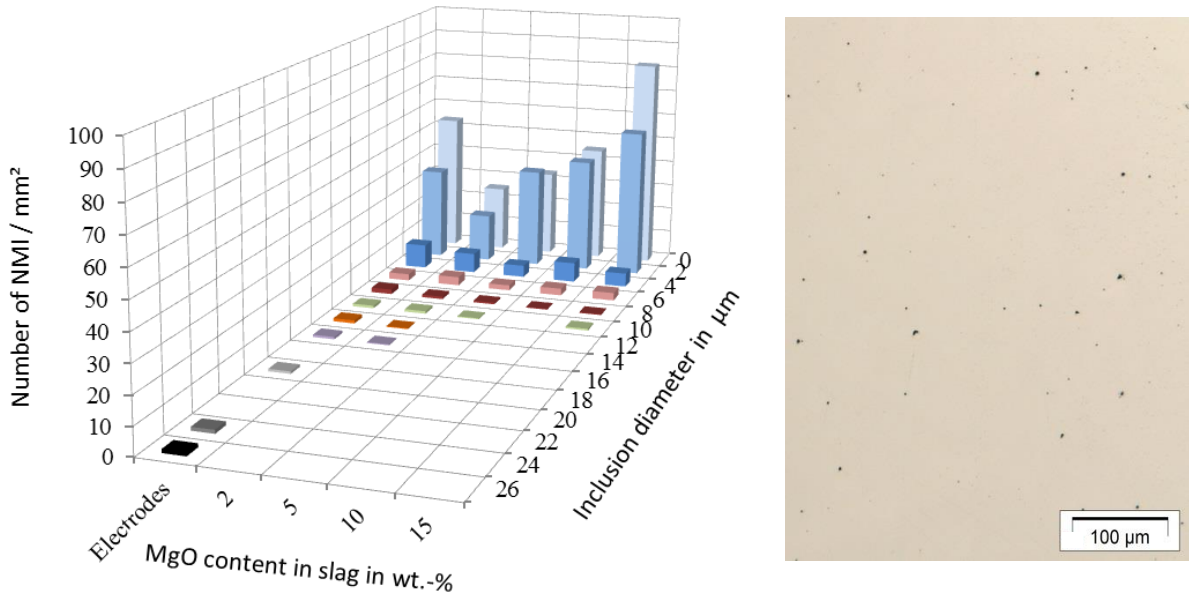

Figure 11. Distribution of NMI (left) and schematic illustration of a prepared sample for inclusion characterization (right)

Regarding the total area of non-metallic inclusions which was determined in fraction of the analyzed image, the high magnesia slag showed similar values as the electrode material due to the high amount of small inclusions. Simultaneously, the average diameter of NMI was found to be the smallest of trials (see Figure 12). All other slag systems resulted in a reduction of the total inclusion area however, the average diameter increased with lowering the MgO amount.

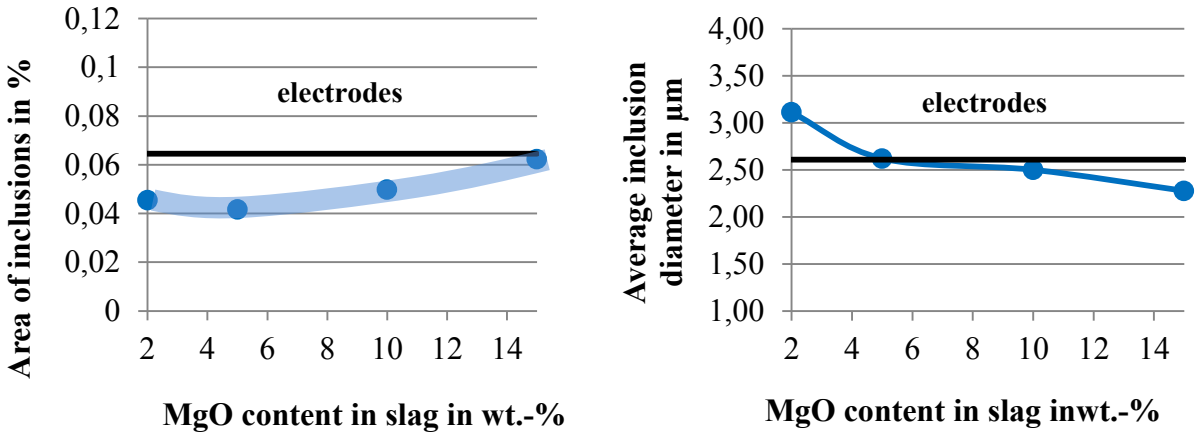

Figure 12. Total area (left) and average diameter (right) of NMI after remelting depending on slag composition

5. Conclusions

- remelting using MgO containing slags was successfully performed and no instabilities were observed
- the electrical resistance was found be dominated by the amount of alumina present in the slag and thus it was decreased by raising the MgO content
- the slag skin thickness increased with raising magnesia amounts in the slag
- as a result of metal-slag interaction, a pick-up of aluminum and a loss of silicon were detected which were nearly independent from the investigated slag composition
- only a strong reduction of the alumina content in the slag resulted in slightly reduced Al amounts dissolved in the metal but compared to the electrode values the contents were still increased
- the analyzed amounts of total oxygen were in the range of the electrode level and could not be further reduced
- desulphurization was successfully performed using all investigated slag systems and a slight decrease of desulphurization capability was observed with increasing ingot height
- large non-metallic inclusions were successfully removed by ESR
- with regard to an inclusion diameter between 4-16 µm, MgO addition led to a higher cleanliness level
- the number of small inclusions (< 4µm) increased when the amount of magnesia was raised

6. Acknowledgement

The authors would like to thank ALD Vacuum Technologies GmbH for the scientific and financial support of this work.

References

[1] Radwitz, S., Scholz, H., Friedrich, B., Franz, H.: Influencing the Electroslag Remelting Process by varying Fluorine Content of the utilized Slag, Proceedings of the European Metallurgical Conference, 2015, P. 887-896

[2] Hoyle, G.: Electroslag Processes - Principles and Practice, Applied Science Publishers LTD, London and New York, 1983

[3] Giesselmann, N.: Numerical simulation of the electroslag remelting process in order to determine influencing parameters on ingot defects, Proceedings of the 1st International Conference on Ingot Casting, Rolling and Forging, 2012

[4] Zhmoidin, G.I., Chatterjee, A.K.: The Phase Diagram of the System $CaO-Al_2O_3-CaF_2$, Journal of Materials Science, 1973, Vol. 25, P. 93-97

[5] Korp, J., Schneider, R., Presoly, P., Krieger, W.: Experimentelle Bestimmung der spezifischen elektrischen Leitfähigkeit hoch CaF_2-haltiger Schlacken, Teil II: Ergebnisse aus Labor und industrieller Praxis, BHM Berg- und Hüttenmännische Monatshefte, 2008, Vol. 5, 153, P. 175-181

[6] Salt, D.J.: Selection of fluxes for electroslag remelting, International Symposium on Electroslag Consumable Electrode Remelting and Casting technology, Pittsburgh, 1967

[7] Bhat, G.K.: A manufacturing program for the electroslag melting and casting of materials, National Technical Information Service U.S. Department of Commerce, 1971

[8] Mitchell, A.: The use of rare-earth oxides in electroslag remelting, Report to: The Molybdenum Corporation of America, 1976